CHAPTER 7

Estimation of Column Calibration Factor and Force Parameters to Predict Temperature Dependence of Thermal Diffusion Factor of Some Simple Molecules

Estimation of Column Calibration Factor and Force Parameters to Predict Temperature Dependence of Thermal Diffusion Factor of Some Simple Molecules

7.1. Introduction

The theoretical thermal diffusion factor as derived from Chapman-Enskog gas kinetic theory[1], based on spherical molecule with spherically symmetric potential field is generally not in good agreement with the experimental α_T's of a binary nonisotopic or even isotopic gas mixture. It is still of special interest from the technical point of view to enrich rare as well as ordinary isotopes. The close correlation between the theoretical α_T's with the intermolecular forces may conveniently be used as an effective tool to investigate the molecular force parameters ε_{ij}/k and σ_{ij} where ε_{ij} is the depth of the potential well, k is the Boltzmann constant and σ_{ij} is the molecular diameter as the process of thermal diffusion unlike viscosity is a second order effect.

Although, TD column was supposed not to yield the actual α_T values both in trend and in magnitude with respect to temperature and composition of the mixture, still it is far superior to any other α_T measuring instruments like two bulbs and trennschaukel as the equilibrium separation factor q_e defined by $q_e=(x_i/x_j)_{top}/(x_i/x_j)_{bottom}$ is very large even in the case of isotopic gas mixture where the mass difference between the components *i* and *j* is practically very small. x_i and x_j are the mass or mole fractions of the lighter (i) and the heavier (j) molecules respectively. The equilibrium separation factor q_e of any binary gas mixture is usually determined for different compositions of a gas mixture at a fixed temperature $\overline{T}$ or for mixture of fixed composition at different experimental temperatures. With the help of q_e thus measured at different pressures well below and around one atmosphere, α_T of a gas mixture could be ascertained. The existing method to evaluate the experimental α_T from $\ln q_e$ measured in a column at different pressures is usually involved with Maxwell and Lennard-Jones model dependent as well as model independent Slieker column shape factors.

In order to obtain the actual α_T of a binary gas mixture, a large number of

workers[2-5] has, however, introduced a scaling factor F_s called the column calibration factor (CCF) for a TD column in the relation:

$$\ln q_{max} = \alpha_T F_s (r_{cold}, r_{hot}, L, \bar{T}) \quad \ldots\ldots\ldots\ldots (7.1)$$

where r_{cold} and r_{hot} are the cold and hot wall radii of a column of geometrical length L. $\bar{T}$ is the mean temperature of the gas mixture defined by $\bar{T}=(T_{hot}+T_{cold})/2$, T_{hot} and T_{cold} are the hot and cold wall temperatures in K respectively. F_s is supposed to be a molecular model independent parameter and entirely depends on the geometry of a TD column.

Roos and Rutherford[6] had measured the pressure dependence of $\ln q_e$ of Kr^{80}-Kr^{86}, Xe^{129}-Xe^{136}, CO^{28}-CO^{29}, $CH_4{}^{16}$-$CH_4{}^{17}$ and $N_2{}^{28}$-$N_2{}^{29}$ with their natural isotopic abundances at two experimental temperatures in K in a hot wire TD column of L=487.7 cm, r_{cold}=0.9525cm and r_{hot} = 0.0795 cm respectively. The measured $\ln q_e$ at different pressures in atmosphere by Roos and Rutherford[6] were plotted in Figs. 7.2 and 7.3 by least square fitted curves with the estimated *a'* and *b'* values at two available temperatures. The *a'* and *b'* for the third temperature were also obtained and the variation of $\ln q_e$ at that temperature is, however, selected for each of them and shown in Figs. 7.2 and 7.3 by dotted curves.

From the known and reliable α_T values[7] as well as experimentally determined $\ln q_{max}$ of Ar^{36}-Ar^{40}, F_s for a column as was derived by Datta and Acharyya[4] was first carried out to yield the temperature dependence of α_T of Kr^{80}-Kr^{86} as

$$\alpha_T = 0.0453\text{-}11.0479 \times 1/\bar{T} \quad \ldots\ldots\ldots\ldots (7.2)$$

The corresponding α_T's at the required experimental temperatures $\bar{T}$ = 455.5, 530.5 and 680.5K in the column of Roos and Rutherford[6] were then obtained. They are shown in Table 7.1. These values together with the experimentally estimated $\ln q_{max}$ of Kr^{80} - Kr^{86} from the curves of $\ln q_e$ vs p as shown elsewhere[8] at those temperatures were then utilised to arrive at the probable temperature dependence of F_s for a column[6] :

$$F_s = 67.1066 - 0.15809\,\bar{T} + 3.29153 \times 10^{-4}\,\bar{T}^2 \quad \ldots\ldots\ldots\ldots (7.3)$$

which is shown graphically in Fig 7.1. The values of F_s together with the corresponding experimental lnq_{max} at any temperature gives us α_T's of the different systems from eq. (7.1). The force parameters ε_{ij}/k and σ_{ij} were estimated from the comparative study of the probable temperature dependence of α_T and C^*_{ij} (12-6 Lennard-Jones potential) with respect to $1/\bar{T}$ and $1/\bar{T}^*$ respectively where $\bar{T}^* = \bar{T}/(\varepsilon_{ij}/k)$. The temperature dependence of α_T could not be predicted with α_T's measured at only two experimental temperatures. Nevertheless, an approximate middle temperature is, however, essential to be selected to reveal the actual variation of α_T's of those systems under consideration with respect to temperature in consistent with the estimation of the actual force parameters among the molecules.

The experimental α_T's for these systems by the existing methods, involved with column shape factors due to Maxwell model[9] and Slieker,[10] as presented in Table 7.2, were obtained and shown graphically in Figs. 7.4-7.8. The theoretical α_T's based on elastic and inelastic collisions were also computed with the estimated force parameters ε_{ij}/k and σ (Table 7.2) and are shown in Figs. 7.4-7.8 for comparison with experimental α_T's. The data thus obtained are, however, shown in Table 7.1 together with the other essential data. The

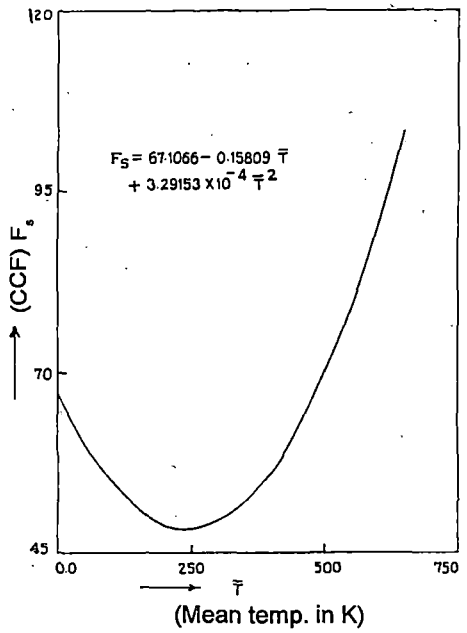

Fig. 7.1. Variation of column calibration factor F_s (CCF) against temperature in K.

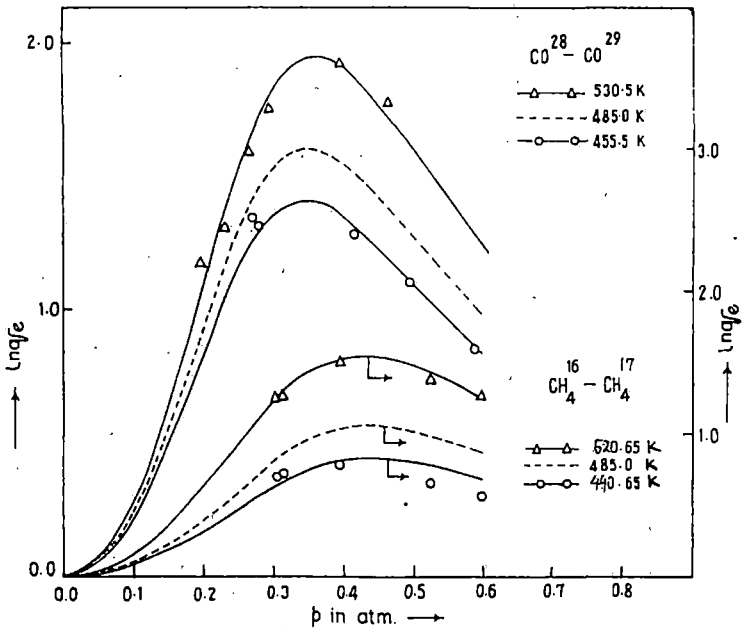

Fig. 7.2. Variation of Inq_e against pressure p in atmosphere: -Δ-Δ- Experimental Inq_e at $\overline{T}$= 530.5K for CO^{28}–CO^{29}, ----- Predicted Inq_e at $\overline{T}$=485K for CO^{28}–CO^{29},–o–o– Experimental Inq_e at $\overline{T}$=455.5K for CO^{28}-CO^{29}, -Δ-Δ- Experimental Inq_e at $\overline{T}$=520.65K for CH_4^{16}–CH_4^{17}, ---- Predicted Inq_e at $\overline{T}$=485 K for CH_4^{16}– CH_4^{17}, –o–o– Experimental Inq_e at $\overline{T}$= 440.65 K for CH_4^{16}– CH_4^{17}.

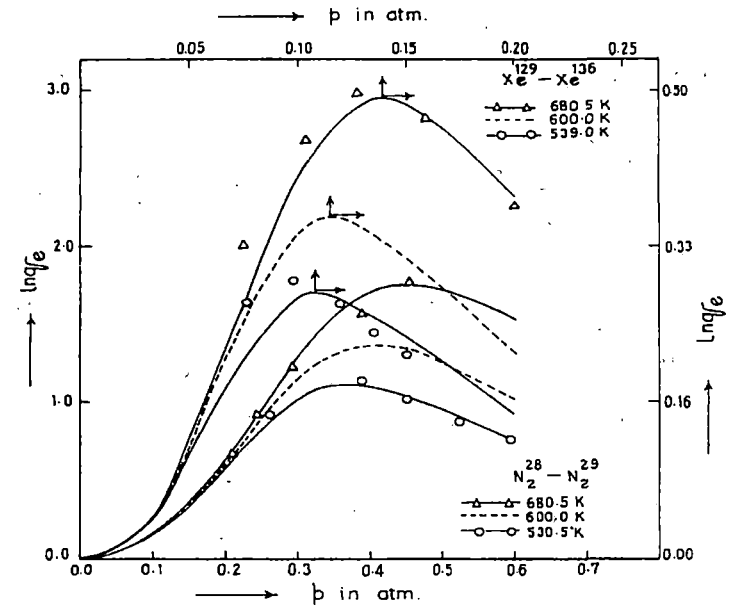

Fig. 7.3. Variation of Inq_e against pressure p in atmosphere: -Δ-Δ- Experimental Inq_e at $\overline{T}$= 680.5K for Xe^{129}–Xe^{136}, ----- Predicted Inq_e at $\overline{T}$= 600.0K for Xe^{129}–Xe^{136},-o-o- Experimental Inq_e at $\overline{T}$= 539.0K for Xe^{129}– Xe^{136}. -Δ-Δ- Experimental Inq_e at 680.5K for N_2^{28}–N_2^{29}. --- Predicted Inq_e at $\overline{T}$=600.0K for N_2^{28}– N_2^{29}. –o–o– Experimental Inq_e at $\overline{T}$= 530.5 K for N_2^{28}– N_2^{29}.

CCF method together with the technique of simultaneous determination of force parameter is thus found to be successful in predicting the exact, reliable and correct temperature variation of α_T of a binary isotopic mixture.

The curves of α_T's against $\bar{T}$ in Figs 7.4-7.8, however, support the possibility of estimation of binary interactions among the molecules as one obtains those from the viscosity of gases and gas mixtures. The estimation of α_T's by the present CCF method are found to be in close agreement so far trends are concerned, as observed in Figs 7.4-7.8, with the theoretical ones in terms of the estimated force parameters (Table 7.2). Thus the methodology so far extended is really a simple, straightforward and unique one.

7.2. Mathematical Formulation to Estimate the Experimental α_T

Both ends being closed for an ideal column of length L, $\ln q_e$ of a gas mixture at any temperature $\bar{T}$ is given by[11]

$$\ln q_e = HL/(K_c + K_d) \qquad \text{..... (7.4)}$$

where H, K_c and K_d are the functions of transport coefficients of a gas mixture. They are proportional to p^2, p^4 and p^0 respectively, p being pressure in atmosphere. In order to remove parasitic remixing effect, Furry and Jones[11] simply added a term K_p called remixing coefficient, being proportional to p^4 to the denominator of eq (7.4). Hence eq (7.4) finally becomes

$$\ln q_e = \frac{a'p^2}{b' + p^4} \qquad \text{..... (7.5)}$$

or, $$p^2/\ln q_e = b'/a' + (1/a')\, p^4 \qquad \text{..... (7.6)}$$

a' and b' are, however, related by

$$(HL/KC)\, p^2 = a' (1 + K_p/K_c)$$

and $$(K_d/K_c)\, p^4 = b' (1 + K_p/K_c)$$

The constants a' and b' were, however, estimated by fitting eq. (7.6) with the

Table 7.1. Experimental and theoretical thermal diffusion factors α_T of binary isotopic mixtures of simple gases with temperatures in K.

Column used	System	Hot wall Temp. (T_{hot}) in K	Cold wall Temp. (T_{cold}) in K	Mean Temp. in K $\bar{T}=\frac{T_{hot}+T_{cold}}{2}$	a' $(atm)^2$	b' $(atm)^4$	Computed $\ln q_{max}$ from eq(7.15)	Column Calibration factor F_ϕ (CCF)
L=Length of the column =487.7 cm	Kr	623	288	455.5	0.0622	0.00055	1.333	63.586
		773	288	530.5	0.1007	0.00074	1.855	75.869
		1073	288	680.5	0.2464	0.00143	3.252	111.94
	Xe	790	288	539	0.0066	0.00014	0.280	77.562
		912	288	600	0.0099	0.00019	0.362	90.748
		1073	288	680.5	0.0187	0.00036	0.492	111.94
Hot wall radius r_{hot} = 0.0795 cm	CO	623	288	455.5	0.3336	0.0142	1.398	63.586
		682	288	485	0.3919	0.0149	1.603	67.858
		773	288	530.5	0.5028	0.0166	1.951	75.869
Cold wall radius r_{cold} = 0.9525 cm	CH_4	593.15	288.15	440.65	0.3414	0.0376	0.886	61.357
		682.00	288.00	485.00	0.4768	0.0361	1.255	65.858
		753.15	288.15	520.65	0.6059	0.0340	1.643	74.023
	N_2	773	288	530.5	0.3156	0.0201	1.115	75.869
		912	288	600	0.4423	0.0265	1.360	90.748
		1073	288	680.5	0.7311	0.0437	1.707	111.94

Column used	System	Estimated α_T using			Computed theoretical α_T	
		Present method	Maxwell shape factor	Slieker shape factor	Elastic	Inelastic
L=Length of the column =487.7 cm	Kr	0.0210	0.0134	0.0146	0.0107	
		0.0245	0.0165	0.0184	0.0127	
		0.0291	0.0252	0.0290	0.0150	
	Xe	0.0036	0.0010	0.0018	0.0087	
		0.0040	0.0018	0.0021	0.0096	
		0.0044	0.0022	0.0025	0.0102	
Hot wall radius r_{hot} = 0.0795 cm	CO	0.0221	0.0100	0.0113	0.0052	0.2861
		0.0236	0.0107	0.0117	0.0057	0.3104
		0.0257	0.0114	0.0127	0.0061	0.3334
Cold wall radius r_{cold} = 0.9525 cm	CH_4	0.0144	0.0070	0.0076	0.0036	0.0230
		0.0191	0.0086	0.0095	0.0046	0.0296
		0.0222	0.0099	0.0110	0.0054	0.0342
	N_2	0.0147	0.0065	0.0073	0.0090	0.4010
		0.0150	0.0069	0.0078	0.0094	0.4081
		0.0153	0.0077	0.0088	0.0102	0.4148

experimentally observed $\ln q_e$ at different pressures in atmosphere. Both a' and b' are now the experimental parameters to govern the variation of $\ln q_e$ against pressure as shown graphically in Figs. 7.2 and 7.3 for CO^{28} - CO^{29}, CH_4^{16} - CH_4^{17} and Xe^{129}- Xe^{136}, N_2^{28}-N_2^{29} respectively with the experimental data[6,8] placed on them at two available temperature. The third temperature would then be selected from the plot of $\alpha_T = A + B/\bar{T}$ with the measured α_T's at two temperatures.

In each case as observed in Figs. 7.2 and 7.3, $\ln q_e$ increases gradually with pressure and assumes maximum value $\ln q_{max}$ at a pressure $p=(b')^{1/4}$ for which $\frac{\delta}{\delta p}(\ln q_e)= 0$. Hence from eq. (7.5) we have

$$\ln q_{max} = \frac{a'}{2\sqrt{b'}} \qquad \text{.....(7.7)}$$

Now a' and b', in Table 7.1, help us fix the values of $\ln q_{max}$ from eq (7.7) and hence the experimental α_T's for the above mentioned systems could, however, be determined from eq.(7.1) with F_s. To use the existing method with Maxwell and Slieker column shape factors eq (7.4) also becomes

$$\ln q_{max} = \frac{HL}{2\sqrt{K_c K_d}} \qquad \text{.....(7.8)}$$

when $\frac{\delta}{\delta p}(\ln q_e) = 0$. The final expression of the experimental α_T's in terms of the column shape factors are finally given by :

$$\alpha_T = 2.39 \times \frac{r_{cold} - r_{hot}}{L} \times \frac{\bar{T}}{\Delta T} \ln q_{max} \cdot \frac{\sqrt{k'_c k'_d}}{h'} \qquad \text{.....(7.9)}$$

and

$$\alpha_T = 2.00 \times \frac{r_{cold}}{L} \cdot \frac{\bar{T}}{\Delta T} \ln q_{max} \frac{\{\pi(1-a^2)[S.F]_3\}^{1/2}}{[S.F]_1} \qquad \text{.....(7.10)}$$

respectively, where the symbols used are of usual significance as mentioned elsewhere[9,10]. The column shape factors which are supposed to take into

account the inherent asymmetry of the column geometry are presented in Table 7.2. The computed α_T's with Maxwell and Slieker column shape factors (Table 7.2) are placed in Table 7.I and shown graphically in Figs 7.4-7.8 by curve No. 2 and 3 respectively in order to compare with those by the present CCF and theoretical ones.

7.3. Derivation of Force Parameters

The principal contribution[12] to the temperature dependence of $\alpha_{T\ theor}$ comes from the factor $(6C^*_{ij} - 5)$ of Chapman-Enskog expression[1] where

$$\alpha_{T\ theor} = g(6C^*_{ij} - 5). \qquad \text{..... (7.11)}$$

The term $(6C^*_{ij} - 5)$ contains only unlike interactions among the molecules. The other part i.e., *'g'* depends on the composition of the gas mixture. Althogh, *'g'* depends slowly on temperature it can be taken fairly constant for a short range of temperature and for a fixed composition of the gas mixture as in the case of the present investigation. It is seen that[13]

$$\alpha_{T\ expt} = A + B/\bar{T} \qquad \text{..... (7.12)}$$

where A and B are two arbitrary constants. C^*_{ij} of eq. (7.11) can also be written as a function of reduced temperature $\bar{T}^*$

$$C^*_{ij} = C + D/\bar{T}^* \qquad \text{..... (7.13)}$$

C and D are two new constants. Now from eqs. (7.11) and (7.13) we have

$$\alpha_{T\ theor} = \left[(6C - 5) + \frac{6D}{\bar{T}^*}\right] g. \qquad \text{..... (7.14)}$$

When $\alpha_{T\ theor} = \alpha_{T\ expt}$ we may write from eqs. (7.12) and (7.14)

$$(6C - 5)g = A. \qquad \text{..... (7.15)}$$

The experimental α_T's at two available temperatures by the CCF method are now used to get the values of A and B. Similarly with the reported C^*_{ij} vs $\bar{T}^*$ curve[14] for 12- 6 Lennard-Jones potential within a short range of reduced temperature $\bar{T}^*$, C and D of eq. (7.13) were easily evaluated. (6C–5) and A could yield *'g'* which enable one to locate the value of C^*_{ij} and T^*; and hence ε_{ij}/k.

This sort of evaluation was further improved by taking into account the small variation of *'g'* with temperature. This was done by repeating the entire procedure as mentioned earlier to get the exact value of *'g'* with the initially estimated ε_{ij}/k and hence the exact value of ε_{ij}/k is finally located. The ε_{ij}/k thus estimated agrees well with the literature values as shown in Table 7.2 for molecules Ar, Kr, Xe, CO, CH_4 and N_2 respectively. With these ε_{ij}/k, the respective σ_{ij}'s were also determined from available viscosity data and are placed in Table 7.2 together with the literature values.

7.4. Theoretical Formula to Estimate $\alpha_{T\,theor}$

(i) **Elastic :** The $\alpha_{T\,theor}$ due to Chapman-Enskog is already given by eq (7.11) which consists of two factors :

$$g = \frac{1}{6[\lambda_{ij}]_1} \cdot \frac{s^{(i)}x_i - s^{(i)}x_j}{X_\lambda + Y_\lambda} \text{ and } (6C^*_{ij} - 5).$$

The first factor is the complicated functions of composition, thermal conductivities of gas and gas mixture while the second one is strongly a temperature dependent term. The symbols used are described in detail in MTGL[1]. The $\alpha_{T\,theor}$ thus computed with ε_{ij}/k and σ_{ij} (Table 7.2) are presented in the 13th column of Table 7.1 and shown graphically in Figs 7.4-7.8 for comparison with $\alpha_{T\,expt}$ by existing and the present CCF method.

(ii) **Inelastic :** According to Monchick *et. al*[15] the $\alpha_{T\,theor}$ due to inelastic collisions is given by :

$$\alpha_{T\,theor} = \frac{(6C^*_{ij} - 5)\mu_{ij}}{5nk[D_{ij}]_1}\left[\frac{\lambda^{\alpha}_{j\,trans}}{x_j M_j} - \frac{\lambda^{\alpha}_{i\,trans}}{x_i M_i}\right] +$$

$$\frac{1}{5nk[D_{ij}]_1}\left[\frac{(6\widetilde{C}^*_{ij} - 5)\lambda^{\alpha}_{j\,int}}{x_j} - \frac{(6\widetilde{C}_{ij} - 5)\lambda^{\alpha}_{i\,int}}{x_i}\right] \qquad \text{..... (7.16)}$$

where the symbols used have their usual meanings[15]. The collision integral ratio $\widetilde{C}_{ij}$ which differs from C^*_{ij}, is very sensitive to inelastic collision and not

symmetric with respect to the interchange of the indices *i* and *j*. The exact value of $\lambda^{\alpha}_{j\,trans}$ or $\lambda^{\alpha}_{i\,trans}$ for a pure gas is given by[15]

$$\lambda^{\alpha}_{j\,trans} = \frac{\eta}{M}\left[\left(\frac{5}{2} C_{v\,trans} + \frac{\rho D_{int}}{\eta} C_{int}\right)\right.$$

$$-\left(\frac{2}{\pi}\cdot\frac{C_{int}}{Z_{rot}}\right)\left(\frac{5}{3}-\frac{\rho D_{int}}{\eta}\right)^{2}$$

$$\left.\left\{1+\frac{2}{\pi Z_{rot}}\left(\frac{5}{3}\frac{C_{int}}{R}+\frac{\rho D_{int}}{\eta}\right)\right\}^{-1}\right] \qquad \text{..... (7.17)}$$

Hence, C_v = 3R/2 = the constant value of translational heat capacity, Z_{rot} = rotational translational collision number for inelastic collision. To evaluate the nonspherical part of eq (7.16) we used Hirschfelder-Euken expression[15] to calculate the internal thermal conductivity λ^{α}_{int} from :

$$\lambda^{\alpha}_{i\,int} = \frac{n[D_{ij}]_1 C_{int}}{1+(x_j / x_i)(D_{ii} / D_{ij})} \qquad \text{..... (7.18)}$$

The inelastic $\alpha_{T\,theor}$ for CO^{28}-CO^{29}, $CH_4{}^{16}$-$CH_4{}^{17}$ and $N_2{}^{28}$-$N_2{}^{29}$ were calculated from eq (7.16) with the help of eqs (7.17) and (7.18). The mass density ρ_{ij}, the coefficient of viscosity η_{ij} and the diffusion coefficient D_{ij} of the gas mixtures were calculated from MTGL[1], in terms of the evaluated ε_{ij}/k and σ_{ij} (Table 7.2). The $\alpha_{T\,theor}$ (inelastic) thus calculated for CO, CH_4 and N_2 isotopic mixtures are placed in Table 7.1 and shown graphically in Figs 7.6-7.8 for comparison.

7.5. Results and Discussions

The least square fitted equations of $p^2/\ln q_e$ against p^4 were worked out from the pressure dependence of experimental $\ln q_e$[6] for Kr^{80}-Kr^{86}, Xe^{129}-Xe^{136}, CO^{28}-CO^{29}, $CH_4{}^{16}$-$CH_4{}^{17}$ and $N_2{}^{28}$-$N_2{}^{29}$ with their natural isotopic abundances. In case of later four systems $\ln q_{max}$ were estimated in terms of a' and b' at two available experimental temperatures. The pressure dependence of $\ln q_e$ at any

intermediate temperature could, however be obtained from the temperature dependence of both α_T and F_s of eqs(7.12) and (7.3). The linearity of b' with a short range of temperature fixes b' and hence a' from eq (7.7) at the intermediate temperature. The pressure dependence of $\ln q_e$ in the selected intermediate

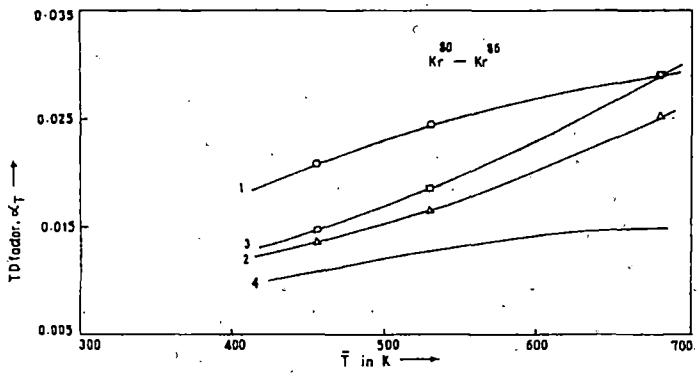

Fig.7.4 Plot of α_T's against $\bar{T}$ in K for Kr^{80}–Kr^{86}. –o–o– Curve 1: Experimental α_T from F_s and $\ln q_{max}$. –△–△– Curve 2: Experimental α_T using Maxwell shape factors. –□–□– Curve 3: Experimental α_T using Slieker shape factors. Curve 4: Theoretical α_T based on elastic collision.

temperature for all the systems except Kr^{80}-Kr^{86} are shown in Figs. 7.2 and 7.3 by dotted lines. The least square fitted equations of $p^2/\ln q_e$ against p^4 at all the temperatures for the aforesaid binary mixtures are given by :

i) Kr^{80}-Kr^{86};

$p^2/\ln q_e = 0.0088 + 16.0771 p^4$ at 455.5 K

$= 0.0074 + 9.9602\ p^4$ at 530.5 K

$= 0.0058 + 4.0584\ p^4$ at 680.5 K

ii) Xe^{129}-Xe^{136};

$p^2/\ln q_e = 0.0212 + 151.515\ p^4$ at 539.0 K

$= 0.0192 + 101.0101\ p^4$ at 600.0 K*

$= 0.0192 + 53.4759\ p^4$ at 680.5 K

iii) CO^{28}-CO^{29};

p^2/lnq_e= 0.0426 + 2.9976 p^4 at 455.5 K

= 0.0382 + 2.5517p^4 at 485.0 K*

= 0.0330 + 1.9888 p^4 at 530.5 K

iv) CH_4^{16}-CH_4^{17};

p^2/lnq_e= 0.1101 + 2.9291p^4 at 440.65 K

= 0.0757 + 2.0973 p^4 at 485.0 K*

= 0.0561 + 1.6504 p^4 at 520.65K

v) N_2^{28}-N_2^{29};

p^2/lnq_e= 0.0637 + 3.1686 p^4 at 520.5 K

= 0.0599 + 2.2609 p^4 at 600.0 K*

= 0.0598 + 1.3678 p^4 at 680.5 K

*Intermediate temperature.

The experimental α_T's due to Maxwell and Slieker column shape factors were placed in the 10th and 11th columns of Table 7.1 and are shown graphically by curve Nos. 2 and 3 respectively in Figs. 7.4-7.8 as a function of temperature. They are almost of the same trends with those of CCF method as evident in Table 7.1 and Figs 7.4-7.8, although, the Slieker column shape factors are very crude in comparison with those of Maxwell inverse fifth power potential model.

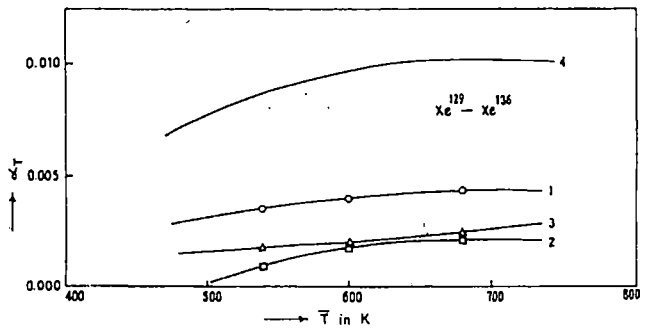

Fig.7.5. Plot of α_T's against $\bar{T}$ in K for Xe^{129}–Xe^{136}. -o-o- Curve 1: Experimental α_T from F_s and lnq_{max}. -□-□- Curve 2: Experimental α_T using Maxwell shape factors. -Δ-Δ- Curve 3: Experimental α_T using Slieker shape factors. Curve 4: Theoretical α_T based on elastic collision.

Table 7.2. Maxwell's model dependent and Slieker's model independent column shape factors, coefficient of viscosity η_{ij} and Diffusion coefficient D_{ij} together with estimated force parameters ϵ_{ij}/k and molecular diameters σ_{ij} used in the calculation of α_T of simple isotopic gas mixtures

System	Model Potential	Estimated		Reported		Mean Temp. ($\bar{T}$) in K
		ϵ_{ij}/k in K	σ_{ij} in Å	ϵ_{ij}/k in K	σ_{ij} in Å	
Ar^{36}–Ar^{40}	LJ 12-6	125.03	3.516	125.2* 119.5**	3.405*	371.0 378.0 387.5
Kr^{80}–Kr^{86}	LJ 12-6	199.55	3.712	199.2* 166.7**	4.020*	455.5 530.5 680.5
Xe^{129}–Xe^{136}	LJ 12-6	228.20	4.253	222.2* 229.0**	4.362*	539 600 680.5
CO^{28}–CO^{29}	LJ 12-6	200.56	3.620	110.0†	3.590†	455.5 485.0 530.5
CH_4^{16}–CH_4^{17}	LJ 12-6	323.28	3.360	148.9* 310.0*	3.630*	440.65 485.00 520.65
N_2^{28}–N_2^{29}	LJ 12-6	80.963	3.914	95.2* 91.5*	3.341*	530.5 600.0 680.5

System	Model Potential	Column shape factors						$\eta_{ij} \times 10^5$ gm cm^{-1} sec^{-1}	D_{ij} cm^{-1} sec^{-1}
		Maxwell			Slieker				
		h'	k_c'	k_d'	$[S \cdot F]_1 \times 6.1$	$\pi(1-a^2)$	$[S \cdot F]_3 \times 9.1$		
Ar^{36}–Ar^{40}	LJ 12-6								
Kr^{80}–Kr^{86}	LJ 12-6	1.015	2.05	0.8143	1.2165	3.121	0.7702	28.53	
		1.225	3.00	0.7829				32.25	
		1.580	4.81	0.7571				39.01	
Xe^{129}–Xe^{136}	LJ 12-6	1.251	3.105	0.7804				33.61	
		1.405	3.85	0.7679				36.62	
		1.579	4.81	0.7571				40.39	
CO^{28}–CO^{29}	LJ 12-6	1.015	2.05	0.8143				24.17	0.4157
		1.095	2.40	0.8000				25.45	0.4629
		1.225	3.00	0.7829				27.33	0.5499
CH_4^{16}–CH_4^{17}	LJ 12-6	0.965	1.84	0.8229				12.58	0.3639
		1.095	2.40	0.8000				13.77	0.4379
		1.195	2.85	0.7857				14.68	0.5009
N_2^{28}–N_2^{29}	LJ 12-6	1.225	3.00	0.7829				33.31	0.6742
		1.405	3.85	0.7679				35.85	0.8293
		1.580	0.81	0.7571				38.97	1.0141

* Maitland *et al.* (1981).
** Hirchfelder *et al.* (1964).
† G. Vasaru (1975).

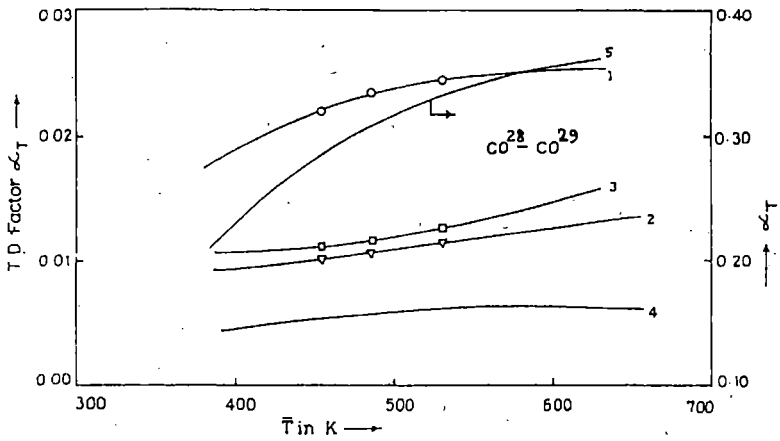

Fig.7.6. Plot of α_T's against $\bar{T}$ in K for CO^{28}–CO^{29}. –o–o– Curve 1: Experimental α_T from F_s and $\ln q_{max}$. –△–△– Curve 2: Experimental α_T using Maxwell shape factors. –□–□– Curve 3 Experimental α_T using Slieker shape factors. Curve 4: Theoretical α_T based on elastic collision. Curve 5: Theoretical α_T based on inelastic collision.

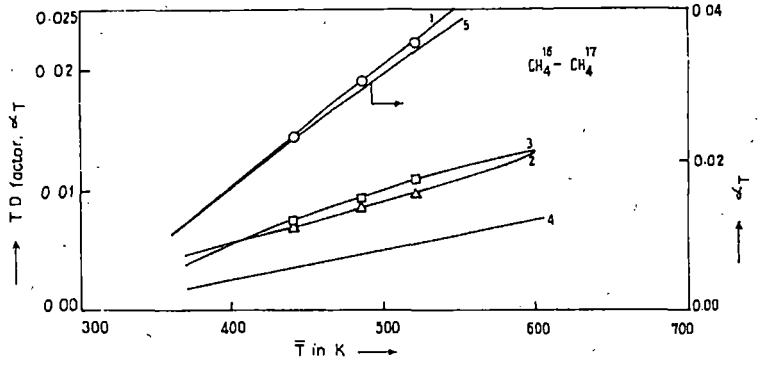

Fig.7.7. Plot of α_T's against $\bar{T}$ in K for CH_4^{16}–CH_4^{17}. –o–o– Curve 1: Experimental α_T from F_s and $\ln q_{max}$ –△–△– Curve 2: Experimental α_T using Maxwell shape factors. –□–□– Curve 3: Experimental α_T using Slieker shape factors. Curve 4: Theoretical α_T based on elastic collision. Curve 5: Theoretical α_T based on inelastic collision.

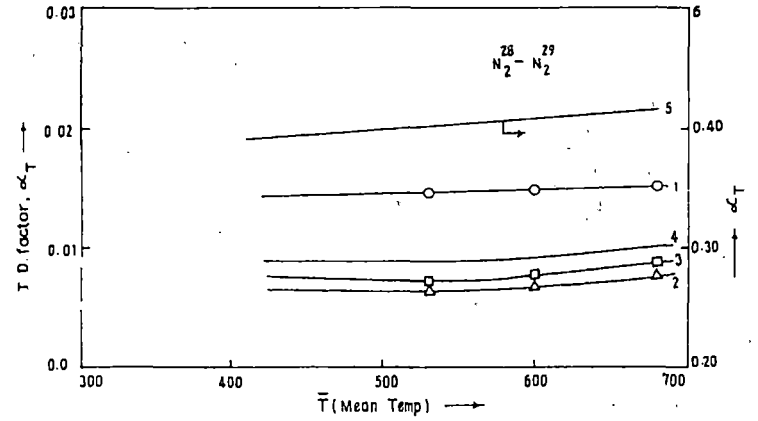

Fig.7.8. Plot of α_T's against $\bar{T}$ in K for N_2^{28}–N_2^{29}. –o–o– Curve 1: Experimental α_T from F_s and $\ln q_{max}$. –△–△– Curve 2: Experimental α_T using Maxwell shape factors. –□–□– Curve 3: Experimental α_T using Slieker shape factors. Curve 4: Theoretical α_T based on elastic collision. Curve 5: Theoretical α_T based on inelastic collision.

The experimental α_T's as obtained in terms of lnq_{max} and F_s from eqs (7.1) and (7.3) are placed in the 9th column of Table 7.1 and shown graphically by the curve No. 1 in all the Figs 7.4-7.8. These are slightly higher than those due to Maxwell (curve 2) and Slieker (curve 3), but exhibit the similar trends as mentioned earlier.

The reliability of the temperature dependence of the experimental α_T's by the CCF method of the aforesaid binary mixtures is, however, ensured with the determination of the respective molecular force parameter ε_{ij}/k's and σ_{ij}'s for the molecules. The estimated force parameters seem to be sensitive to intermolecular interactions and agree excellently well for Ar, Kr, and Xe while for CO, CH_4 and N_2 they deviate remarkably. Both ε_{ij}/k's and σ_{ij}'s are all presented in columns 3 and 4 to compare with the literature values placed in columns 5 and 6 respectively of Table 7.2. This fact at once suggests the existence of inelastic collisions in the later three isotopic mixtures. It was, however, pointed out by some workers[16, 17] that the theory of inelastic collision effect in thermal diffusion is not widely applicable except for eccentrically loaded sphere molecule as one of the component in binary mixtures. The simple theory so far adopted here to estimate the force parameters is based on the elastic collision amongst the molecules. The inelastic collision in molecules like CO, CH_4 and N_2 may be the reason of such deviations (Table 7.2.).

The α_T's due to elastic collision theory from eq. (7.11) in terms of ε_{ij}/k and σ_{ij} are also shown graphically by the curve no 4 of Figs. 7.4-7.8 for comparison with α_T's by CCF method. They are placed in the 12th column of Table 7.1. The graphs in Figs, 7.4-7.8 and Table 7.1, clearly show that in case of Kr and Xe elastic α_T's almost coincide with α_T's by CCF method so far the magnitudes and trends are concerned. But in case of CO, CH_4 and N_2 elastic α_T's are of one order smaller in magnitudes and not with the same trends with α_T's from CCF method.

The fact as mentioned above indicates that Chapman Enskog gas kinetic theory[1] could not interprete the variation of α_T's of CO, CH_4 and N_2 isotopic mixtures with temperature probably due to the presence of inelastic collision among such molecules as shown in Tables 7.1 and 7.2. But the theory appears

to be successful to explain the temperature dependence of α_T's of spherically symmetric molecules like Ar, Kr, and Xe as evident from Tables 7.1 and 7.2 and Figs 7.4 and 7.5.

The α_T based on inelastic collisions as derived by Monchick *et al*[15] from eq (7.16) for CO^{28}-CO^{29}, CH_4^{16}-CH_4^{17} and N_2^{28}-N_2^{29} are presented in column 13 of Table 7.1. They are plotted graphically by the curve No. 5 in Figs 7.6-7.8 for comparison.

From all the discussions we may conclude that α_T's as obtained by CCF method is a simple, straightforward and unique one. This study further indicates that the nature of variation of F_s is the same as observed earlier,[2-4, 17] but differing in the magnitudes of coefficients A, B and C in $F_s = A + B\bar{T} + C\bar{T}^2$. Thus the nature of variation of F_s with temperature $\bar{T}$(Fig 7.1) confirms that the CCF method to locate the magnitude and trend of α_T in Figs 7.4-7.8 is correct.

7.6. Conclusions

Although, F_s is supposed to be an essential tool in determining the experimental α_T in a column measurement, still the functional relationship of F_s with r_{cold}, r_{hot}, L and $\bar{T}$ remains unexplored. Simultaneous determination of F_s and the force parameters seems to be an important step forward to observe α_T of both isotopic and nonisotopic binary mixtures of simple molecules as a function of temperature. A rigorous study of experimental F_s through experimentally determined $\ln q_{max}$ of binary mixture having accurate α_T is needed with different column geometries to serve this purpose.

The very existence of inelastic collision effects in thermal diffusion of suitable molecules forming binary mixture have to be studied in detail through $\ln q_{max}$ and F_s to improve the theory of inelastic collision effects in thermal diffusion.

References

[1] J. O. Hirchfelder, C. F. Curtiss and R. B. Bird: *Molecular Theory of Gases and Liquids* (John Willey and Sons, New York, 1964) p. 541.

[2] S. Acharyya, A.K. Das, P.Acharyya, S.K. Datta and I. L. Saha : J. Phys. Soc. Jpn. **50** (1981) 1603.

[3] S. Acharyya, I.L. Saha, P. Acharyya, A. K. Das and S. K. Datta : J. Phys. Soc. Jpn. **51** (1982) 1469.

[4] A. K. Datta and S. Acharyya : J. Phys. Soc. Jpn. **62** (1993) 1527.

[5] J. L. Navarro, J. A. Madariage and J M. Saviron : J. Phys. Soc. Jpn. **50** (1983) 1603.

[6] W. J. Roos and W. M. Rutherford : J. Chem. Phys. **50** (1969) 3936

[7] F. Vandervolk : Ph. D. Dissertation (1963).

[8] I. Yamamoto, H. Makino and A. Kanagawa : J. Nucl. Sci. Technol. **27** (1990) 156.

[9] G. Vasaru : *Thermal Diffusion Column, supplied by S. Raman* (B.A.R.C., Bombay).

[10] C. J. G. Slieker : Z. Naturforsch. **20** (1965) 591.

[11] W. H. Furry and R. C. Jones, Phys. Rev. **69** (1946)459.

[12] B. N. Srivastava and K. P. Srivastava : Physica, **23** (1957) 103.

[13] R. Paul, A. J. Howard and W. W. Watson : J. Chem, Phys. **39** (1963) 3053.

[14] M. Klein and F. J. Smith : Tables of collision integral for the (m,6) potential for the values of m, Arnold Engineering Development Centre, Tennessee, 1968.

[15] L. Monchick, S. I. Sandlar and E. A. Mason : J. Chem. Phys. **49** (1968) 1178.

[16] T. K. Chattopadhyay and S. Acharyya : J. Phys. B **7** (1974) 2277.

[17] G. Dasgupta, A. K. Datta and S. Acharyya : Pramana **43** (1994) 81..